Published in final edited form as:
Int J Cancer. 2013 May 15; 132(10): 2258–2269. doi:10.1002/ijc.27917.

Ovarian Cancer Cells, not Normal Cells, Are Damaged by Mirk/Dyrk1B Kinase Inhibition

Jing Hu, **Holly Deng**, and **Eileen A. Friedman**
Pathology Department, SUNY Upstate Medical Univ., Syracuse, NY, 13210

Abstract

Prior studies had shown that the Mirk/dyrk1B gene is amplified/upregulated in about 75% of ovarian cancers, that protein levels of this kinase are elevated in quiescent G0 cells, and that Mirk maintains tumor cells in quiescence by initiating rapid degradation of cyclin D isoforms and by phosphorylation of a member of the DREAM complex. Depletion of Mirk/dyrk1B led to increased cyclin D levels, an elevated ROS content, and loss of viability. However, many normal cells in vivo are quiescent, so targeting a kinase found in quiescent cells might be problematic. In the current study, Mirk kinase activity was found to be higher in ovarian cancer cells than normal cells. Pharmacological inhibition of Mirk/dyrk1B kinase increased cyclin D levels both in quiescent normal diploid cells and in quiescent CDKN2A-negative ovarian cancer cells, but led to more active CDK4/cyclin D complexes in quiescent ovarian cancer cells, allowing them to escape G0/G1 quiescence, enter cycle with high ROS levels and undergo apoptosis. The ROS scavenger N-acetyl cysteine reduced both the amount of cleaved PARP and the extent of cancer cell loss. In contrast, normal cells were spared because of their expression of CDK inhibitors that blocked unregulated cycling. Quiescent early passage normal ovarian epithelial cells and two strains of quiescent normal diploid fibroblasts remained viable after inhibition of Mirk/dyrk1B kinase, and the few cells that left G0/G1 quiescence accumulated in G2+M. Thus inhibition of Mirk kinase targeted quiescent ovarian cancer cells.

Keywords

quiescence; ovarian cancer; Mirk; Dyrk1B; ROS

INTRODUCTION

The Minibrain/dyrk protein kinase family member Mirk/dyrk1B (1), (2), (3) is an effector for both oncogenic K-ras and H-ras through a Rac1 to MKK3 pathway, and also can be activated by cellular stresses like the chemotherapeutic drug 5-fluorouracil which activates MKK3 (4), (5), (6), (7). Mirk expression levels are very low in most normal cell types except for skeletal muscle (8), suggesting that this kinase has a non-critical function in most normal cells. Mirk is upregulated or amplified in a large subset of ovarian cancers compared with normal ovarian tissue (9). Mirk is one of 16 genes within a consistently amplified 660 kb subregion of the 19q13 amplicon found in pancreatic cancers (10), and ovarian cancers (11), suggesting selection for this gene. Mirk depletion leads to increased ROS levels in pancreatic cancer and in colon cancer cells (12). Similarly, depletion of Mirk in each of four ovarian cancer cell lines increased their intracellular levels of ROS, sensitizing them to cisplatin which itself raises ROS levels (13). The combined effect of Mirk depletion and low

Address correspondence to: Eileen Friedman, Ph.D., SUNY Upstate Medical University Department of Pathology, 2305 Weiskotten Hall, 750 East Adams Street, Syracuse, New York 13210; Tel: 315-464-7148; FAX 315-464-8419; friedmae@upstate.edu.

cisplatin levels was sufficient to kill the tumor cells, suggesting that Mirk may be an attractive target in ovarian cancers (13). However, subsequent studies showed that Mirk levels varied widely during cell cycling with the greatest protein levels found in ovarian cancer cells made quiescent by serum-starvation or growth to high cell density (9). A re-examination of the experimental conditions in the cisplatin studies revealed that several were performed in serum-free culture or over a several day growth period which led to high cell density (9) suggesting that most of the ovarian cancer cells were quiescent when Mirk-depletion sensitized them to cisplatin. The significance of quiescence to Mirk response was troubling since many normal cells in the body are quiescent, except the hematopoietic system and the gut epithelium. When a Mirk kinase inhibitor was tested on pancreatic and colon cancer cells in a recent study (14), normal non-immortalized epithelium from either of these human tissues was not studied in parallel, as such tissue is not readily available and is difficult to maintain in tissue culture. In contrast, normal, non-immortalized ovarian diploid epithelial cells are commercially available and can be cultured. In the current study the effects of pharmacological inhibition of Mirk kinase are compared in these normal ovarian cells, two diploid fibroblast strains and in ovarian cancer cells under culture conditions where cells entered a reversible quiescent state.

METHODS & MATERIALS

Materials

Cell lines and strains were obtained from the ATCC, and fresh cells were taken from frozen stocks negative for mycoplasma, on average every 3 months. In May of 2012, STR (short tandem repeat) profiling of 14 and 15 loci, respectively, was used to authenticate the SKOV3 and TOV21G cell lines. Reversible quiescence in culture was induced by serum-starvation for 3 days, with the cells able to enter cycle when fresh nutrients were added, as confirmed by flow cytometry to measure cell movement from G0 to mitotic arrest by nocodazole (13),(9). Early passage human ovarian epithelial cells isolated from human ovarian tissue (cryopreserved primary or passage one cultures, ScienCell) were cultured in serum-free, growth factor containing ovarian epithelial cell medium (OEpiCM, ScienCell) by the provider's instructions, and made quiescent by culture in serum-free DMEM where over 60% were found in G0. Flow cytometry after propidium iodide staining and western blotting were performed as detailed (9), with antibodies to cleaved caspase-3 (#9661) from Cell Signaling, agarose conjugate to CDK4 sc-23896AC, sc-8396 to cyclin D1, sc-182 to cyclin D3, sc-528 to p27, and sc-1616 to actin from Santa Cruz, and to phosphorylated H2AX from Trevigen. For determination of DNA and RNA content to distinguish G0 from G1 cells, two parameter cell cycle analysis was performed on cells fixed in ice-cold 70% ethanol, then washed. Hoechst 33258 was added to bind to DNA and block DNA staining by Pyronin Y, followed by Pyronin Y to bind to RNA exactly as detailed (12). Mirk kinase inhibitor RO5454948 was provided by Hoffmann La Roche, Nutley, N.J. Its chemical structure, similar IC_{50} values on purified dyrk1B and the closely related dyrk1A, selectivity in a screen of 49 protein kinases, and biological effects on pancreatic and colon cancer cells were recently reported (14). RO5454948 only effected cell cycling in colon cancer cells if Mirk/dyrk1B was expressed, having no effect on the cycling of HCT116 colon cancer cells which express only dyrk1A, while leading more SW620 colon cancer cells, which express both dyrk1B and dyrk1A, to enter cycle and incorporate BrdU (14).

Mirk kinase assay

Log phase cells or cells made quiescent by serum-free culture for 4 days were lysed in modified ice cold RIPA buffer called IP buffer (50mM Tris-HCl pH 7.5, 150 mM NaCl, 1% NP40, 10% glycerol, 1 protease inhibitor tablet (Roche), and phosphatase inhibitor cocktails 1 and II diluted from 100X stocks). 300 ug lysate was incubated with 2 ug/5μl anti-Mirk

C'terminal peptide polyclonal antibody overnight at 4°, 20μl protein G-agarose added for 2 hr at 4°. The agarose complexes were washed 3X with IP buffer, then 3X with kinase buffer (50mM Tris-HCl pH7.5, 10 mM $MgCl_2$, 1 mM DTT). Incubation continued for 15 min at 30°C in 20μl kinase buffer containing 50μM cold ATP, 5μCi ^{32}P-γATP, 2 μg myelin basic protein substrate. The reaction was stopped by addition of 2X SDS sample buffer and boiling. Samples were analyzed by SDS-PAGE on 12% acrylamide gels, followed by autoradiography and western blotting for Mirk.

ROS measurements

total ROS was measured by DCFA metabolism, ROS superoxide levels weremeasured by dihydroethidium fluorochrome metabolism, and nitric oxide levels measured by diaminofluorescein (DAF) metabolism. Cells were plated at 4×10^5 per 6 well plate, changed to serum-free DMEM and treated with 0.5μM RO5454948 for 1,2 or 3 days, with a fresh media change daily.

RESULTS

Quiescent ovarian cancer cells have higher levels of Mirk/dyrk1B protein and are more sensitive to Mirk kinase inhibition than proliferating cells

Quiescent tumor cells are generally more resistant to chemotherapeutic drugs and radiation than cycling cells, and can repopulate the tumor in a favorable microenvironment. A drug targeting quiescent tumor cells could have clinical utility. Mirk and p130/Rb2 were shown to mediate quiescence in ovarian cancer cells by depletion studies (9). Quiescence is maintained by the DREAM complex (p130/Rb2, E2F4, DP1 and a stable core including the LIN52 protein), which disassembles when cells leave quiescence and enter cycle. In quiescent cells Mirk/dyrk1B and the closely related Dyrk1A phosphorylate the core protein LIN52 at a site necessary for its quiescence function (15). Mirk also blocks cells in quiescence by initiating cyclin D turnover by phosphorylation at an ubiquitination site conserved in all isoforms (16). TOV21G, SKOV3 and OVCAR3 ovarian cancer cells could serve as model cell lines to study drug targeting in quiescent cells because these lines were shown to enter a viable reversible quiescent state when deprived of growth factors, while other ovarian cancer lines such as OVCAR4 underwent cell death by autophagy (9).

As a first step, quiescent cultures were confirmed to contain a high proportion of G0 cells and a low proportion of S phase cells. Two parameter flow cytometry for both DNA and RNA was used to distinguish G1 cells from G0 cells, which have lower RNA levels because of polyribosome degradation. G0 cells and S phase cells were 75% and 1%, respectively, in quiescent TOV21G cultures, while 17% and 26% of cells in cycling cultures were in G0 and S, respectively (Fig. 1A). SKOV3 cultures exhibited similar distributions, as seen earlier (9).

Mirk/dyrk1B is an unusual kinase in that its expression and protein abundance vary widely during the cell cycle, with low levels in S phase because of downregulation through MEK/Erk signaling (17), and significant upregulation when cells enter G0/early G1 quiescence (18), (9). Since Mirk/dyrk1B protein levels were upregulated 3 to 4 fold in the quiescent ovarian cancer cultures (Fig. 1A), we asked whether inhibition of this kinase would have greater toxicity in quiescent cultures. When quiescent, both TOV21G cultures (Fig. 1A) and SKOV3 cultures (data not shown) were 2 to 3 fold more sensitive to pharmacological inhibition of Mirk by the small molecule inhibitor RO5454948, with EC_{50} levels of 0.8–0.9μM, compared with about 2μM for proliferating cells. We next examined whether the decreased cell number after Mirk kinase inhibition was due to growth arrest or induction of apoptosis.

The ability of ovarian cancer cells to escape quiescence and enter cycle after Mirk kinase inhibition was examined by flow cytometry

Many cell manipulations are required for two parameter flow cytometry, which could cause loss of sub-G0/G1 apoptotic cells, so analysis of ovarian cancer cells was carried out by one parameter flow cytometry, measuring DNA content after propidium iodide staining. Both TOV21G and SKOV3 cells were observed to slip out of quiescence into cycle when treated with the Mirk inhibitor at about their EC_{50} levels, as shown by an increased fraction of S and G2+M cells. This was more pronounced in the p53null SKOV3 cells compared with the p53 wild-type TOV21G cells. However, sub-G0/G1 apoptotic cells (arrows, Fig. 1B) were observed after 2–4 days of treatment of both lines with the Mirk kinase inhibitor. By 4 days apoptotic cells comprised 15–25% of the either tumor cell population. These lines differ in cell cycle regulators which control G0 to G1 to S cycling, with TOV21G wild-type in p53, expressing p21 but not p16, and SKOV3 p53null expressing neither p21 or p16 (19), (20), (21), (data not shown). Since SKOV3 cells express fewer CDK inhibitors, it may be easier for SKOV3 cells than TOV21G cells to traverse G1, enter S prematurely and die, after release from G0 quiescence by Mirk inhibition.

Cancer cells express higher Mirk protein levels and kinase activity. Would normal diploid cells exhibit less response to Mirk kinase inhibition because they expressed little Mirk protein? TOV21G, SKOV3 and OVCAR3 ovarian cancer cells, the HD and BJ strains of normal diploid fibroblasts, and normal ovarian epithelial cells in early passage were made quiescent by serum starvation, and their Mirk protein levels and Mirk kinase activities determined. The cancer cells had 2–17 fold higher levels of Mirk protein than the normal diploid cells (Fig. 1C). The OVCAR3 cells with a 20-fold amplified Mirk gene (9) expressed the most Mirk protein. Kinase activity was determined by an in vitro kinase assay of immunoprecipitated Mirk on the exogenous substrate MBP, and then normalized to the amount of immunoprecipitated Mirk (Fig. 1C, lower panel; note that twice as much Mirk protein was present in SKOV3 cells than the normal epithelium (upper panel) so SKOV3 cells had twice the total kinase activity). Since Mirk kinase activity was higher in the cancer cells than the normal diploid cells, pharmacological inhibition of Mirk might lead to larger changes in the cancer cells.

Mirk kinase inhibition has little effect in normal diploid cells. Many normal cells in the body are quiescent, so targeting Mirk might allow them to escape quiescence. Normal diploid ovarian epithelial cell cultures were made quiescent by culture in serum-free medium and treated with the Mirk inhibitor for 2 and 3 days (Fig. 2A). The major effect of Mirk kinase inhibition was to enable about 10%-12% of cells to leave G0 (Fig. 2A, arrowheads), and to increase the G2+M cell fraction from about 20% to about 35%. Few cells were seen in S phase. About 70% of cells in the HD strain of normal diploid dermal fibroblast quiescent cultures accumulated in G0 after 4 days of serum starvation, with about 10% fewer G0 cells in Mirk kinase inhibitor-treated parallel cultures (Fig. 1B, arrowheads). Mirk kinase inhibition moved about 8% more cells into G2+M. Thus the Mirk kinase inhibitor slightly reduced the fraction of G0 quiescent diploid epithelial cells and fibroblasts, while the majority of the cells pushed into cycle accumulated in G2+M. Apoptotic sub-G0/G1 cells were not detected.

The ability of normal cells to escape quiescence and become apoptotic after Mirk kinase inhibition was examined by flow cytometry

No sub-G0/G1 apoptotic cells were seen by one parameter flow cytometry after Mirk inhibitor treatment of two strains of human diploid fibroblasts, BJ and HD (Fig. 2C, only 3 day point shown) or normal diploid ovarian epithelial cells (Fig. 2C, day 2 and day3 shown). Possibly the Mirk kinase inhibitor preferentially damaged the cancer cells. To test this

hypothesis, the drug was washed out and cells were placed in fresh growth medium containing the mitotic inhibitor nocodazole to block any cycling cells in G2+M. After wash-out of the drug, normal diploid BJ fibroblasts regained cycling with the same cell cycle distribution as untreated control cells. Mirk inhibitor-treated TOV21G ovarian cancer cells exhibited a slower traverse of the cell cycle, with many cells still in G1 and S phase, while most control cells had cycled into G2+M (Fig. 2D). Many sub-G0/G1 apoptotic cells were seen in the inhibitor-treated TOV21G culture before inhibitor removal, so the slower cycling after release might be due to G1 and S phase checkpoints induced by unrepaired cellular damage. Aberrant control of p130/Rb2 may allow escape of quiescent cancer cells into cycle after Mirk inactivation. Mirk blocks cell cycling in G0/early G1 by phosphorylating cyclin D isoforms at a conserved ubiquitination site, causing their turnover (16). Depletion of Mirk by either of two RNAi duplexes increased cyclin D levels 2–3 fold in both TOV21G and SKOV3 cells (13). As expected, levels of cyclin D rose in both cancer cell lines over 2–4 days of treatment with the Mirk inhibitor (Fig. 3A), but also increased in both BJ and HD diploid fibroblast strains. As a control, an increase in cyclin D content was also seen when Mirk was depleted from both fibroblast strains and from normal ovarian epithelium (Fig. 3B). Mirk depletion was 60% in ovarian epithelium, 71% in BJ cells and over 90% in HD cells.

Total p27 levels rose in only the normal diploid cells, not the cancer cells, after pharmacological inhibition of Mirk kinase in time-course studies (Fig. 3A). The 4 to 5 fold increase in p27 levels after Mirk kinase inhibition was not an off-target effect, as depletion of Mirk by RNAi (Fig. 3B) also increased p27 levels in normal diploid cells. This increase in p27 only in normal cells led to a 2–3 fold increase in p27 bound to CDK4/cyclin D complexes only in normal diploid cells, not in TOV21G or SKOV3 cancer cells (Fig. 3C). These CDK4/cyclin D complexes in normal cells should be inactive, unable to phosphorylate and inactivate the DREAM complex component p130/Rb2 that maintains G0. In fact, treatment of BJ and HD fibroblast strains with the Mirk kinase inhibitor did not decrease the amount of E2F4 co-immunoprecipitated with p130/Rb2 (Fig. 3D), consistent with the lack of escape from G0 shown by most cells (Fig. 2B). In contrast, CDK4/cyclin D complexes in cancer cells treated with the Mirk inhibitor were expected to be more active and capable of phosphorylating p130/Rb2 since cyclin D levels were increased, p27 levels were not increased, and cells did not express p16, and in the case of SKOV3, also did not express p21. Mirk kinase inhibitor treatment of ovarian cancer cells led to slower electrophoretic mobility of p130/Rb2 consistent with increased phosphorylation, with a stronger response in SKOV3 ovarian cancer cells which express fewer CDK inhibitors. In cancer cells this caused disassembly of the DREAM complex, up to a 3-fold loss of sequestered E2F4 (Fig. 3D), and escape from quiescence (Fig. 1B). Depletion of Mirk had a similar effect, leading to increased phosphorylation of p130/Rb2, disassembly of the DREAM complex and loss of sequestered E2F4 (12).Thus both ovarian cancer cell lines tested responded to the Mirk kinase inhibitor by loss of sequestered E2F4 (Fig. 3D) and escape into cycle as seen by flow cytometry analysis (Fig. 1B), while the majority of cells in both strains of normal diploid fibroblasts remained arrested in a reversible quiescent state (Fig. 2B,C). The small shift of both normal diploid fibroblasts and ovarian epithelial cells from G0 into G2 with Mirk kinase inhibitor treatment (Fig. 2A,B) might be due to a subpopulation with increased cyclin D levels, which progressed to a functional G2 checkpoint.

Mirk kinase inhibition has differential effects on viability and on ROS induction. The HD fibroblast strain and TOV21G cancer cells were treated with a series of concentrations of RO5454948 from 0.1 to 5μM and their relative viability then compared. The HD cells were 94%-99% as viable as untreated control cells, while the TOV21G cells lost viability beginning at 0.5μM, with only about 30% viable cells at 1μM (Fig. 4A). In parallel

experiments, relative cell number was estimated by metabolism of MTT. The normal fibroblasts reached a relative cell number about 70% of untreated cultures (Fig. 4B), possibly because the inhibitor blocked some cell cycling in G2+M (Fig. 2B). In contrast, the lowest concentration tested of 0.1μM reduced both SKOV3 and TOV21G cell numbers to about half of untreated controls, while 1μM reduced cell numbers to 17–22% of untreated controls. Thus at 1μM RO5454948, about 99% of normal HD fibroblasts were viable compared with only 30% of the remaining TOV21G cells, as the total cancer cell number had been reduced about 6-fold. In earlier studies, Mirk depletion by RNAi duplexes increased TOV21G cell death by 50% as assayed by dye exclusion, while depletion of Mirk in BJ fibroblasts did not increase the fraction of dead cells (9). Thus inhibition of Mirk kinase activity in normal and cancer cells resulted in similar differential effects on cell viability as did these earlier studies with Mirk depletion (9).

Selective killing of cancer cells by a small molecule targeting the stress response to ROS has been observed (22). Normal cells generally have lower ROS levels than cancer cells, allowing a selective attack on cancer cells. Mirk depletion increases ROS levels in cancer cells, but the role of Mirk kinase in ROS handling in normal cells was not studied (12), (13). Pharmacological inhibition of Mirk kinase increased total ROS levels, as assayed by the DCFA fluorochrome, up to 2-fold both in SKOV3 cells and in TOV21G cells in time-course experiments (Fig. 4C) and in dose-response studies (not shown). A 2-fold increase in total ROS was about the maximum that could be seen when Mirk was depleted from either line, as greater increases in ROS caused cell lysis (13). A roughly 2-fold increase in total ROS in TOV21G cells by a two-day treatment (Fig. 4C) was followed by a loss in cells (data not shown) reflected in less total ROS after 3 days. The Mirk kinase inhibitor also increased ROS levels in the OV90 and OVCAR8 ovarian cancer cell lines, (data not shown). In contrast, no increase in total ROS levels with Mirk kinase inhibition was seen in either HD or BJ normal diploid fibroblasts or normal ovarian epithelium (Fig. 4D). Doxycycline-induced short hairpin-depletion of Mirk in SKOV3 cells decreased expression of superoxide dismutase 2 (13), so Mirk kinase inhibition should increase superoxide levels. Levels of the superoxide class of ROS, detected with the dihydroethidium fluorochrome, increased in both TOV21G and SKOV3 ovarian cancer cells treated over a 3-day period, but did not increase over control levels in either the HD or BJ fibroblast strain (data not shown). The nitric oxide class of ROS species was increased up to 250% in both cancer cell types, but was at control levels in the normal cells after 48 hours of treatment (data not shown). Thus Mirk kinase inhibition increased total ROS levels and the levels of superoxide ions only in SKOV3 and TOV21G cancer cells.

Increased apoptosis markers in cancer cells compared with normal diploid cells. Elevated ROS levels could cause DNA damage reflected in cell cycle checkpoints (Fig. 2D), greater abundance of the DNA damage protein γH2AX, and increased apoptosis. This was observed. Time-course analysis by western blotting demonstrated an increase in the apoptotic proteins cleaved caspase 3 and cleaved PARP, coupled with an increase in the DNA damage protein γH2AX, in TOV21G and SKOV3 ovarian cancer cell cultures after 1–4 days of treatment with the Mirk kinase inhibitor (Fig. 5A). There was no alteration in the amount of Mirk protein by the Mirk kinase inhibitor, as expected. However, there was little increase in either cleaved PARP or cleaved caspase 3 in either strain of diploid fibroblast, compared with SKOV3 cells grown in parallel conditions (Fig. 5A). Note that the BJ and the HD fibroblasts had more actin than SKOV3 cells. The amount of cleaved PARP (normalized to actin) after 3 days of Mirk kinase inhibition in SKOV3 cells was 44 times that in HD fibroblasts and 13 fold that in BJ fibroblasts. Similarly, after 3 days of Mirk kinase inhibition the amount of cleaved caspase 3 in SKOV3 cells was 49 fold higher than in HD fibroblasts and 14 fold that in BJ fibroblasts. Consistent with the differential effects on induction of apoptotic proteins, diploid fibroblasts treated with Mirk inhibitor grew very

slowly, while there was a loss in cell numbers in Mirk inhibitor treated ovarian cancer cultures (data not shown). Analysis of three additional ovarian cancer cell lines, OV90, OVCAR8 and OVCAR4, showed that the Mirk kinase inhibitor increased levels of cleaved PARP, cleaved caspase 3, and γH2AX in each line after 3 days of treatment (Fig. 5B). In sharp contrast, Mirk inhibition induced no increase in the low level of cleaved PARP and no increase in cleaved caspase 3 levels in a strain of normal human ovarian epithelial cells in early passage (Fig. 5C). SKOV3 cells were treated in parallel and lysates run on the same gel for an internal control. Thus in each of 5 ovarian cancer cell lines, the Mirk kinase inhibitor increased apoptosis when tested at concentrations which induced only 2–6% as much apoptosis in two strains of normal diploid fibroblasts or early passage normal ovarian epithelial cells. This strong difference and the relative viability studies (Fig. 4A,B) may indicate a therapeutic window to use Mirk kinase inhibition as part of treatment of ovarian cancers in vivo.

Histone protein H2AX molecules within the chromatin at a double-stranded DNA break site become phosphorylated on a serine near the carboxyl terminus. Many phosphorylated H2AX (γH2AX) molecules are found at such a break, creating a focal site for accumulation of proteins involved in DNA repair and chromatin remodeling within a short time of DNA damage (23). Both the Mirk/dyrk1B kinase inhibitor RO5454948 and Mirk depletion, either by induction of a stably transfected shRNA to Mirk exon 11 or by transient transfection of RNAi duplexes to exon 5, induced doubled-strand DNA breaks identified by γH2AX in quiescent Panc1 pancreatic cancer cells (14). Likewise, Mirk kinase inhibition increased the level of phosphorylated H2AX (γH2AX) in SKOV3 and TOV21G ovarian cancer cells with a maximum after 3 days (Fig. 5A), as if the breaks were repaired or the cells had died and were lost to analysis. Mirk kinase inhibition also increased γH2AX levels in OV90, OVCAR8 and OVCAR4 ovarian cancer cells (Fig. 5B). In both normal diploid fibroblast strains an increase in γH2AX levels were seen after 2 days of inhibitor treatment, followed by almost complete loss after 3 days of treatment, possibly indicating DNA repair or cell loss (Fig. 5A). The Mirk kinase inhibition caused little increase in γH2AX levels in normal ovarian epithelial cells within the first 3 days of treatment, correlating well with the lack of cell death seen by analysis of apoptotic proteins or visual examination of the cultures.

Toxic effects of the Mirk kinase inhibitor due to ROS, and can be reversed by the antioxidant N-acetyl cysteine. SKOV3 and TOV21G cells were treated with the Mirk inhibitor, with one set of cells also treated with N-acetyl cysteine (NAC) to reduce ROS levels. The Mirk inhibitor increased the amount of cleaved PARP several-fold, while addition of NAC led to a dose-dependent decrease in cleaved PARP in both cell types (Fig. 6A). There was no alteration in Mirk or actin protein levels, used as controls. In parallel studies, the number of SKOV3 cells and TOV21G cells remaining after Mirk inhibitor treatment was about one-third of control levels (Fig. 6B). The remaining cells still exhibited some increase in ROS levels over controls, 160% in SKOV3. Concurrent treatment with NAC prevented much of this cell loss, with cell numbers of SKOV3 and TOV21G cultures at 87%(+/−4%) of controls and 117% (+/−13%) of controls, respectively. ROS levels either returned to control levels in SKOV3 cells 116% (+/−4%) or were reduced to 57%+/−9% of control TOV21G cells (Fig. 6B). Analysis of cell growth by MTT analysis gave a similar picture. The Mirk kinase inhibitor reduced relative cell numbers to 10–17% of controls, whereas treatment with the antioxidant N-acetyl cysteine reversing some of the growth inhibition, with relative cell numbers increasing to 30% of control SKOV3 cultures and to 54% of TOV21G control cultures (Fig. 6C). Thus NAC treatment partially reduced ROS levels, enabling more tumor cells to survive treatment with the Mirk kinase inhibitor, and demonstrated that increased ROS levels led to cell death.

DISCUSSION

Mirk/dyrk1B kinase is widely expressed at low levels in most tissues, but is upregulated in several solid tumors including ovarian cancer, pancreatic cancer, non-small cell lung cancers, osteosarcomas and rhabdomyosarcomas (24),(25), (26). Study of Mirk/dyrk1B as a therapeutic target has some unique challenges. First, Mirk/dyrk1B is not mutated in cancer cells, like other kinases such as B-Raf in melanomas or erbB2 in breast cancers. Mirk activity appears proportional to its expression level, which is elevated in many cancers, and is increased by upstream activators such as oncogenic K-ras or H-ras, which initiate a Rac1 to MKK3 to Mirk signaling cascade (4),(5),(7). Second, Mirk/dyrk1B functions primarily in quiescent cells where it is transcriptionally upregulated. Thus the typical xenograft tests are untenable. Under these conditions, tumor cell growth is rapid and Mirk protein levels are quite low (data not shown). No Mirk function is known in cycling cells. Mirk associates in large molecular weight complexes in cells (27), possibly associated with its upstream activator kinases through association with scaffold proteins like Han11 (28), and is known to phosphorylate a member of the DREAM complex which controls cell cycle arrest in quiescence (15). These DREAM complexes dissociate when cells enter cycle and Mirk protein levels fall sharply. Third, the choice of a transgenic mouse model is difficult because many rely on strong promoters, which again keep cells in cycle.

As a result of these limitations, this initial study has compared three ovarian cancer cell lines, one with Mirk gene amplification, with early passage normal ovarian epithelium and two strains of human diploid fibroblasts. These cells can readily be placed into a reversible quiescent state in culture, so Mirk function in these different cell types can be compared. Low Mirk levels (8) and lack of oncogenic ras genes to activate Mirk in normal cells suggests that Mirk will have much weaker activity in most normal cells compared with those cancers in which the Mirk gene is either amplified or Mirk gene expression is upregulated. Supporting this interpretation, 20-fold depletion of Mirk in cultured diploid fibroblasts resulted in little loss of viability (5), (9). Mirk is not an essential gene because embryonic knockout of Mirk/dyrk1B caused no evident phenotype in mice (29). Thus inhibition of Mirk might cause few deleterious effects in normal tissue.

In the current study, treatment with the small molecule Mirk kinase inhibitor R5454948 had a selective effect on quiescent cancer cells expressing elevated levels of active Mirk kinase, allowing the cancer cells to escape quiescence with high ROS levels. These improperly cycling cancer cells died by apoptosis, as shown by appearance of sub-G0/G1 apoptotic cells, increased levels of apoptotic markers and a decrease in cell numbers. Blocking ROS by a chemical antioxidant reduced cell loss, showing the role for elevated ROS in loss of survival capacity. In addition, p53 mutations have been found in almost all high-grade serous ovarian adenocarcinomas, indicating that stress induction of the CDK inhibitor p21 would be minimal, and one-third of cases had very low or no expression of CDKN2A (p16/ink4a) (30). Thus quiescent cancer cells in vivo, like SKOV3 cells in culture, might be able to escape quiescence in response to the increased cyclin D levels caused by Mirk inactivation because the cancer cells lacked sufficient CDK inhibitors. Normal cells would be able to block cycling because of their expression of these CDK inhibitors. The lack of deleterious effects on normal cells by RO5454948 was not limited to this Mirk/dyrk1B inhibitor. Another Mirk inhibitor was administered to athymic mice by intraperitoneal injection over a 2 week period at concentrations up to 10μM, and had no effect on normal cell viability as judged by mouse weight, activity and general appearance (Friedman, manuscript in preparation). Thus Mirk/dyrk1B kinase inhibitors have the novel property of targeting those quiescent cancer cells with high Mirk kinase activity and reduced CDK inhibitor expression.

Acknowledgments

This work was supported by National Institutes of Health Grant 5R21CA135164, the Jones/Rohner Foundation, and the Schoeck-Blakely Ovarian Cancer Research Fund (all to E.F.)

References

1. Tejedor F, Zhu X, Kaltenbach E, Ackermann A, Baumann A, Canal I, Heisenberg M, Fischbach K, Pongs O. Minibrain:a new protein kinase family involved in postembryonic neurogenesis in Drosophila. Neuron. 1995; 14:287–301. [PubMed: 7857639]
2. Kentrup H, Becker W, Heukelbach J, Wilmes A, Schurman A, Huppertz C, Kainulainen H, Joost H-G. Dyrk, a dual specificity protein kinase with unique structural features whose activity is dependent on tyrosine residues between subdomains VII and VIII. J Biol Chem. 1996; 271:3488–95. [PubMed: 8631952]
3. Becker W, Weber Y, Wetzel K, Eirmbter K, Tejedor F, Joost H-G. Sequence characteristics, subcellular localization and substrate specificity of dyrk-related kinases, a novel family of dual specificity protein kinases. J Biol Chem. 1998; 273:25893–902. [PubMed: 9748265]
4. Jin K, Lim S, Mercer SE, Friedman E. The Survival Kinase Mirk/dyrk1B Is Activated through Rac1-MKK3 Signaling. J Biol Chem 2005. Dec 23; 2005 280(51):42097–105.
5. Jin K, Park S-J, Ewton D, Friedman E. The survival kinase Mirk/dyrk1B is a downstream effector of oncogenic K-ras. Cancer Res. 2007; 67:7247–55. [PubMed: 17671193]
6. Jin K, Ewton D, Park S, Hu J, Friedman E. Mirk regulates the exit of colon cancer cells from quiescence. J Biological Chemistry. 2009; 284(34):22916–25.
7. Lauth M, Bergstrom A, Shimokawa T, Tostar U, Jin Q, Fendrich V, Guerra C, Barbacid M, Toftgard R. DYRK1B-dependent autocrine-to-paracrine shift of Hedgehog signaling by mutant RAS. Nat Struct Mol Biol. 2010; 17(6):718–25. [PubMed: 20512148]
8. Lee K, Deng X, Friedman E. Mirk Protein Kinase Is a Mitogen-activated Protein Kinase Substrate That Mediates Survival of Colon Cancer Cells. Cancer Res. 2000; 60(13):3631–7. [PubMed: 10910078]
9. Hu J, Nakhla H, Friedman E. Mirk/dyrk1B and p130/Rb2 mediate quiescence in ovarian cancer cells. International Journal of Cancer. 2011; 129(2):307–18.
10. Kuuselo R, Savinainen K, Azorsa DO, Basu GD, Karhu R, Tuzmen S, Mousses S, Kallioniemi A. Intersex-like (IXL) Is a Cell Survival Regulator in Pancreatic Cancer with 19q13 Amplification. Cancer Res. 2007; 67(5):1943–9. [PubMed: 17332321]
11. Thompson FH, Nelson MA, Trent JM, Guan X-Y, Liu Y, Yang J-M, Emerson J, Adair L, Wymer J, Balfour C, Massey K, Weinstein R, et al. Amplification of 19q13.1–q13.2 sequences in ovarian cancer : G-band, FISH, and molecular studies. Cancer Genetics and Cytogenetics. 1996; 87(1):55. [PubMed: 8646743]
12. Deng X, Ewton DZ, Friedman E. Mirk/Dyrk1B maintains the viability of quiescent pancreatic cancer cells by decreasing ROS levels. Cancer Research. 2009; 69(8):3317–24. [PubMed: 19351855]
13. Hu J, Friedman E. Depleting Mirk Kinase Increases Cisplatin Toxicity in Ovarian Cancer Cells. Genes & Cancer. 2010; 1:803–11. [PubMed: 21113238]
14. Ewton D, Hu J, Vilenchik M, Deng X, Luk K-C, Polonskaia A, Hoffman AF, Zipf K, Boylan JF, Friedman E. Inactivation of Mirk/dyrk1b kinase targets quiescent pancreatic cancer cells. Molecular Cancer Therapeutics. 2011; 10(11):2104–14. [PubMed: 21878655]
15. Litovchick L, Florens LA, Swanson SK, Washburn MP, DeCaprio JA. DYRK1A protein kinase promotes quiescence and senescence through DREAM complex assembly. Genes & Development 2011. Apr 15; 2011 25(8):801–13.
16. Zou Y, Ewton D, Deng D, Mercer S, Friedman E. Mirk/dyrk1B Kinase Destabilizes Cyclin D1 by Phosphorylation at Threonine 288. J Biol Chem. 2004; 279:27790–8. [PubMed: 15075324]
17. Deng X, Ewton DZ, Pawlikowski B, Maimone M, Friedman E. Mirk/dyrk1B Is a Rho-induced Kinase Active in Skeletal Muscle Differentiation. J Biol Chem. 2003; 278(42):41347–54. [PubMed: 12902328]

18. Deng X, Mercer SE, Shah S, Ewton DZ, Friedman E. The Cyclin-dependent Kinase Inhibitor p27Kip1 Is Stabilized in G0 by Mirk/dyrk1B Kinase. J Biol Chem. 2004; 279(21):22498–504. [PubMed: 15010468]
19. D'Andrilli G, Kumar C, Scambia G, Giordano A. Cell cycle genes in ovarian cancer: steps toward earlier diagnosis and novel therapies. Clin Cancer Res. 2004; 10(24):8132–41. [PubMed: 15623586]
20. Fang X, Jin X, Xu HJ, Liu L, Peng HQ, Hogg D, Roth JA, Yu Y, Xu F, Bast RC Jr, Mills GB. Expression of p16 induces transcriptional downregulation of the RB gene. Oncogene. 1998; 16(1): 1–8. [PubMed: 9467937]
21. Flak MB, Connell CM, Chelala C, Archibald K, Salako MA, Pirlo KJ, Lockley M, Wheatley SP, Balkwill FR, McNeish IA. p21 Promotes oncolytic adenoviral activity in ovarian cancer and is a potential biomarker. Mol Cancer. 2010; 9:175. [PubMed: 20598155]
22. Raj L, Ide T, Gurkar AU, Foley M, Schenone M, Li X, Tolliday NJ, Golub TR, Carr SA, Shamji AF, Stern AM, Mandinova A, et al. Selective killing of cancer cells by a small molecule targeting the stress response to ROS. Nature. 2011; 475(7355):231–4. [PubMed: 21753854]
23. Bonner WM, Redon CE, Dickey JS, Nakamura AJ, Sedelnikova OA, Solier S, Pommier Y. GammaH2AX and cancer. Nat Rev Cancer. 2008; 8(12):957–67. [PubMed: 19005492]
24. Friedman E. Mirk/dyrk1B in cancer. Journal of Cellular Biochemistry. 2007; 102:274–279. [PubMed: 17583556]
25. Yang C, Ji D, Weinstein EJ, Choy E, Hornicek FJ, Wood KB, Liu X, Mankin W, Duan Z. The Kinase Mirk is a Potential Therapeutic Target in Osteosarcoma. Carcinogenesis. 2009; 31(4):552–8. [PubMed: 20042639]
26. Friedman E. The kinase Mirk/dyrk1B: a possible therapeutic target in pancreatic cancer. Cancers. 2010; 2(3):1492–512.
27. Zou Y, Lim S, Lee K, Deng X, Friedman E. Serine/Threonine Kinase Mirk/Dyrk1B Is an Inhibitor of Epithelial Cell Migration and Is Negatively Regulated by the Met Adaptor Ran-binding Protein M. J Biol Chem. 2003; 278(49):49573–81. [PubMed: 14500717]
28. Ritterhoff S, Farah CM, Grabitzki J, Lochnit G, Skurat AV, Schmitz ML. The WD40-repeat protein Han11 functions as a scaffold protein to control HIPK2 and MEKK1 kinase functions. EMBO J. 2010; 29(22):3750–61. [PubMed: 20940704]
29. Leder S, Czajkowska H, Maenz B, de Graaf K, Barthel A, Joost H-G, Becker W. Alternative splicing variants of the protein kinase DYRK1B exhibit distinct patterns of expression and functional properties. Biochem J. 2003; 372:881–8. [PubMed: 12633499]
30. Cancer Genome Atlas Research Network. Integrated genomic analyses of ovarian carcinoma. Nature. 2011; 474(7353):609–15. [PubMed: 21720365]

Novelty

Chemotherapeutic drugs and radiation are more toxic to cycling cancer cells than quiescent ones. Quiescent ovarian cancer cells are enriched in Mirk/dyrk1B so pharmacological inhibition of this kinase allows quiescent cancer cells to be targeted. Mirk/dyrk1B inhibition elevated cyclin D levels, allowing cancer cells to escape G0/G1 quiescence and enter cycle with high ROS levels and DNA damage, leading to cell death. Inhibition of the low Mirk/dyrk1B kinase activity in normal quiescent diploid cells had little effect on cell viability, and the few cells that left G0/G1 quiescence accumulated in G2+M.

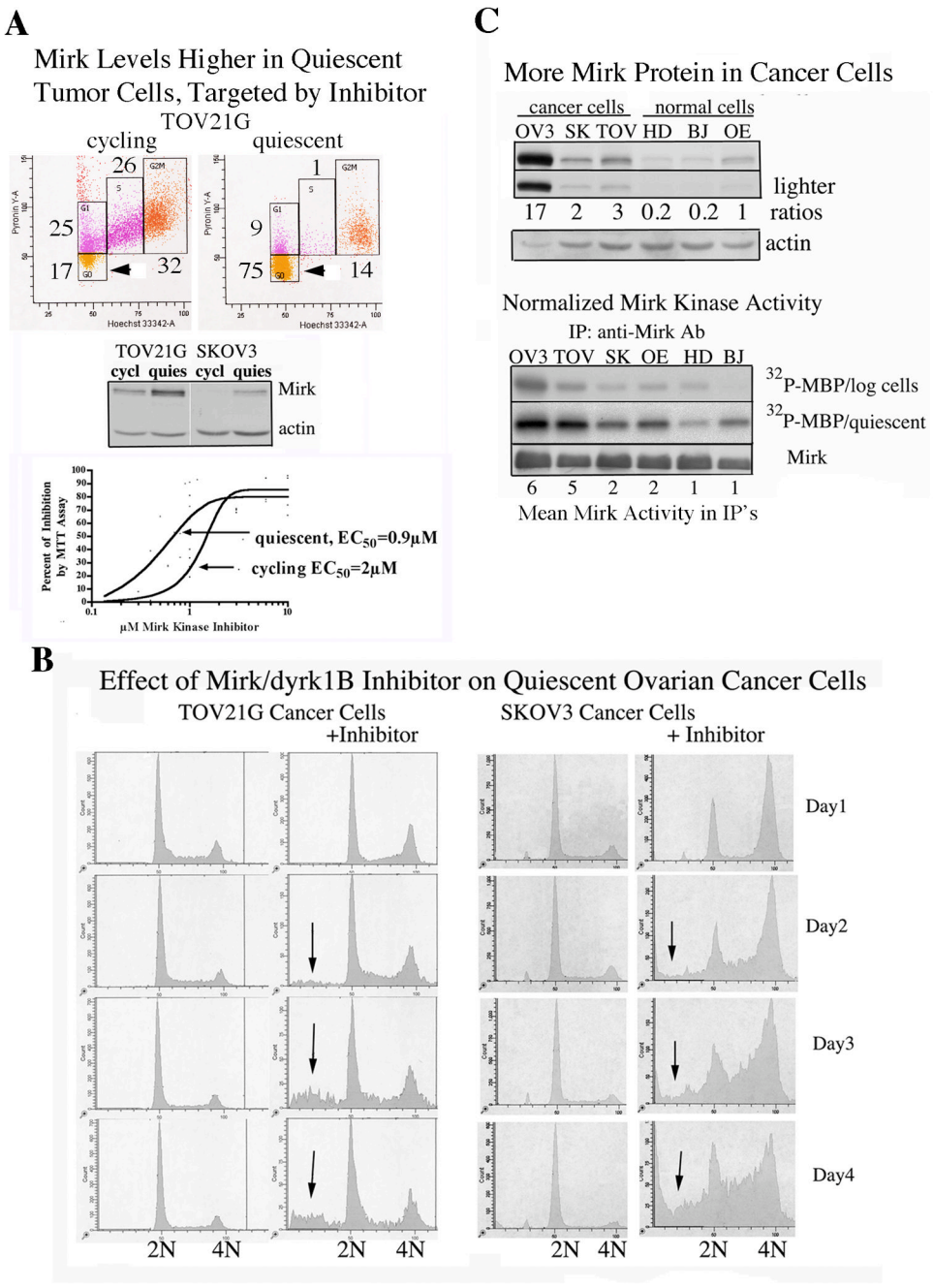

Fig. 1.

Mirk/dyrk1B expression is elevated when ovarian cancer cells become quiescent, making the cells more sensitive to a Mirk kinase inhibitor, which decreases cell numbers by increasing the fraction of sub-G0/G1 apopotic cells.

A. (upper) TOV21G cancer cells were either maintained in log phase growth, or cultured serum-free for 4 days to induce quiescence, and cell cycle position determined by two parameter flow cytometry. Cell cycle fractions were designated as G0 gold (arrowheads); G1 magenta; S purple; G2+M red, as measured by two component analysis by flow cytometry after staining DNA with Hoechst dye and RNA with Pyronin Y. %G0 and %G1 at left, %S above, %G2+M, below in this and all other graphs. (middle) Western blots of

Mirk and actin in quiescent and log phase cycling cultures shown. (lower) TOV21G cells were cultured either in log phase growth or made quiescent, then treated 2 days with a range of concentrations of Mirk kinase inhibitor before measurement of relative cell numbers by MTT metabolism. A mean of 3 experiments were analyzed by GraphPad Prism 4 software and curve fitting with nonlinear regression plotted using the Boltzman sigmoidal dose-response curve, with R squared for the two culture conditions a mean of 0.8856. The mean MTT values for untreated log cells and quiescent cultures were 1013+/−27 and 952+/−61, respectively.

B. The Mirk inhibitor induces cell cycle progression and sub-G0/G1cells in ovarian cancer cell cultures. Log phase TOV21G and SKOV3 ovarian cancer cells were plated at 5×10^5 in 60mm culture dishes and allowed to attach overnight. Media was changed to serum-free DMEM to induce quiescence, with TOV21G and SKOV3 cells treated with 0.5μM and 0.75μM, respectively, Mirk kinase inhibitor. DNA distributions were assayed by one parameter flow cytometry following staining with propidium iodide. Arrows indicate sub-G0/G1 apoptotic cells. One of duplicate experiments shown.

C. Three human ovarian cancer cell lines (OVCAR3, SKOV3, TOV21G), the human diploid fibroblast strains HD and BJ, and early passage human normal ovarian epithelial cells (OE) were made quiescent by culture in serum-free DMEM for 2 days before western blot analysis. (lower panel) Immune complex kinase reaction on myelin basic protein (MBP) of Mirk immunoprecipitated from either log phase or quiescent cultures, with mean Mirk activity normalized to the amount of immunoprecipitated protein below lanes. OVCAR3 cells exhibit a 20-fold amplified Mirk gene and about twice as much Mirk was immunoprecipitated from the OVCAR3 lysate.

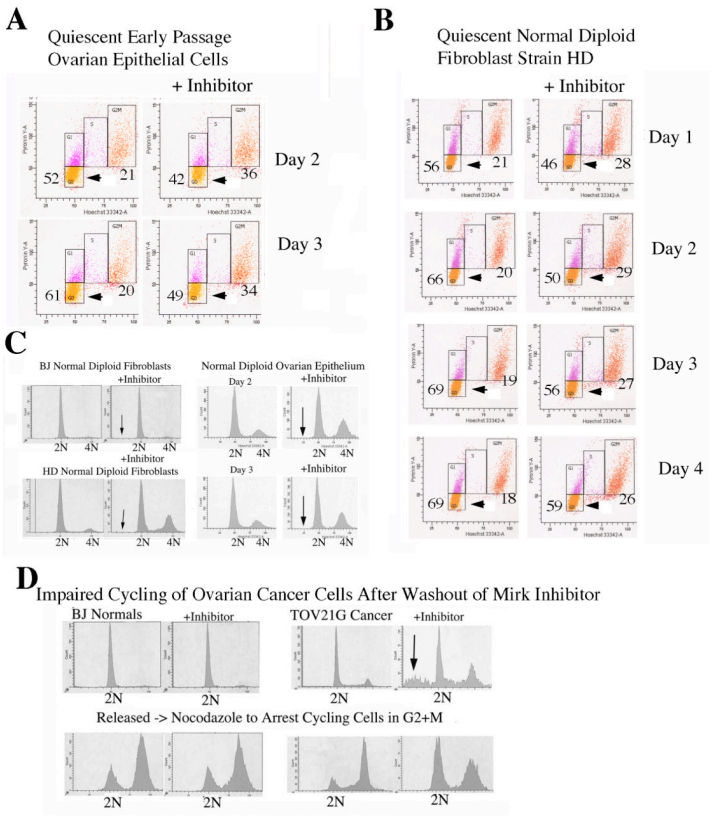

Fig. 2.

The Mirk kinase inhibitor has little effect on normal diploid cells.

A. Early passage normal human diploid ovarian epithelial cells were made quiescent by culture in serum-free ovarian epithelial cell medium (ScienCell), with one set treated with 0.5μM of Mirk kinase inhibitor. G0 (arrows). %G0 and %G2+M cells given after two-parameter flow cytometry. Similar data seen after 1 day treatment.

B. HD normal human diploid fibroblasts were made quiescent by culture in serum-free DMEM for 1 to 4 days, with one set treated with 0.5μM of Mirk kinase inhibitor, and %G0 and %G2+M cells given after two parameter flow cytometry.

C. HD and BJ strains of normal diploid fibroblasts and early passage normal human diploid ovarian epithelial cells were made quiescent by serum-starvation and treated with 0.5μM of Mirk kinase inhibitor for 2 or 3 days, as noted. Cell cycle analysis after propidium iodide staining.

D. TOV21G ovarian cancer cells and the BJ strain of normal diploid fibroblasts were serum-starved for 3 days to induce quiescence with concurrent treatment with 0.5μM Mirk kinase inhibitor as noted. (lower panel) To test for the capacity of cells to re-enter cycle, cells were resuspended in fresh growth medium for 24 hours and cell cycle progression assayed by culture for an additional 24 hours in growth medium containing 50 ng/ml nocodazole to block cycling cells in G2+M. Cell cycle analysis after propidium iodide staining.

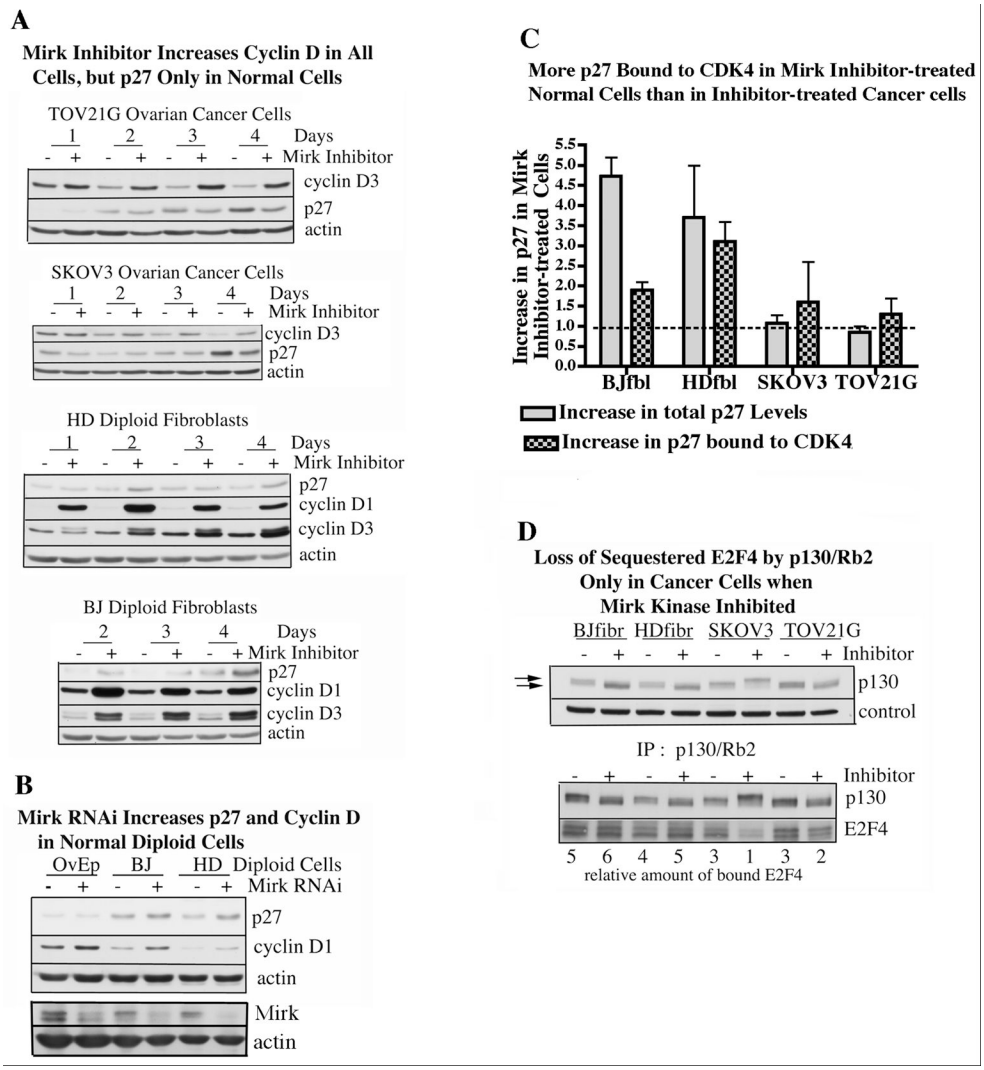

Fig. 3.

Mirk kinase inhibition has differential effects on cell cycle regulators in normal and in cancer cells.

A. The effect of Mirk inhibitor on p27, cyclin D1 and cyclin D3 was determined by western blotting after cells were serum-starved for 1 to 4 days with treatment by addition of 0.5μM Mirk inhibitor as noted. Similar data seen in 3–4 experiments, including ones with normal and cancer cells analyzed on the same gel.

B. HD and BJ strains of normal diploid fibroblasts and early passage normal human diploid ovarian epithelial cells were made quiescent and depleted of Mirk by transfection of RNAi C duplexes as described (13) before analysis of p27 and cyclin D1 levels by western blotting. Additional samples from the same experiment were analyzed for Mirk and actin levels by western blotting. Note that the epithelial cells had higher levels of alpha-actin than the fibroblast strains.

C. HD and BJ strains of normal diploid fibroblasts and TOV21G and SKOV3 ovarian cancer cells were made quiescent and treated with 0.5μM Mirk kinase inhibitor for 3 days, then total p27 and p27 bound to immunoprecipitated CDK4 normalized to amount of immunoprecipitated CDK4 was measured by densitometry of western blots. Mean +/-SE shown (n=3).

D. (upper) The abundance and migration of p130/Rb2 was determined by western blotting after 4 days exposure to Mirk kinase inhibitor at 0.5μM. (lower) immunoprecipitation of p130/Rb2 followed by western blotting for p130/Rb2 and bound transcription factor E2F4. (below) relative abundances of E2F4 co-immunoprecipitated with p130/Rb2.

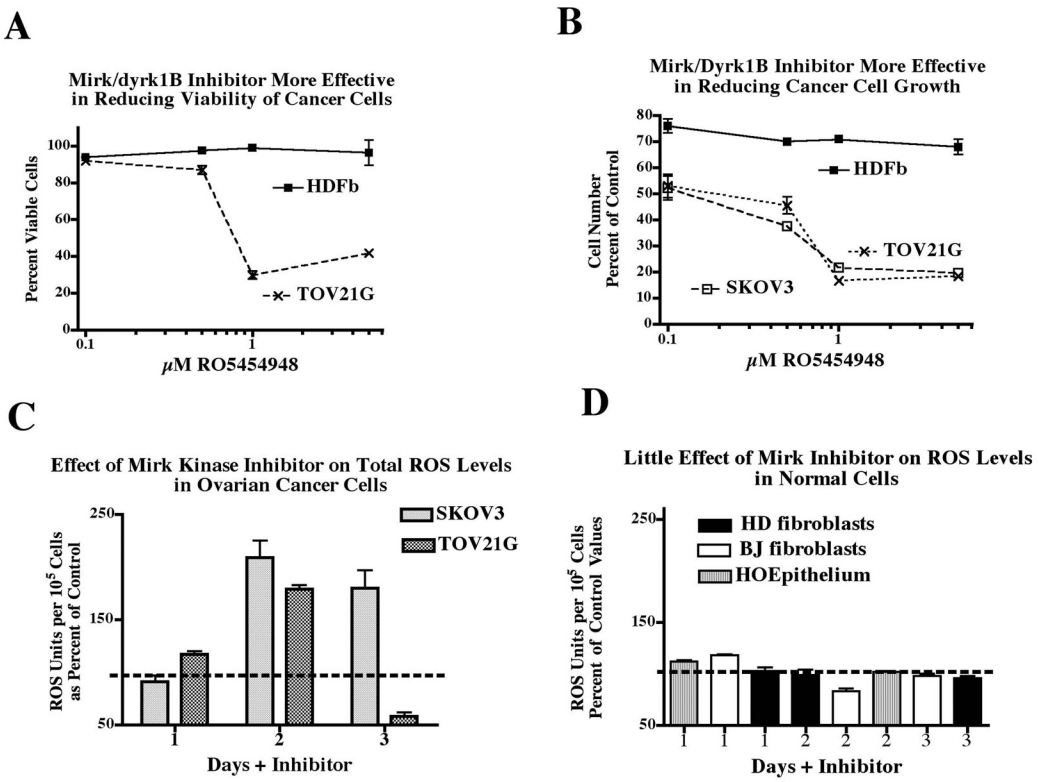

Fig. 4.

The relative decrease in viability and the amount of ROS induced by Mirk kinase inhibition in quiescent normal diploid cells and in cancer cells.

A. The capacity of Mirk kinase inhibitor concentrations from 0.1 to 5μM to kill HD normal human diploid fibroblasts (HDFb) and TOV21G cancer cells was compared by trypan blue exclusion. 5×10^4 cells were plated per 6 well plate and maintained in DMEM+0.2%FBS for 8 days. A mean of 315 cells was assayed for each data point (n=2, +/−SD if >5%). The control values were set to 100%.

B. Parallel plates to panel A were assayed by MTT metabolism (n=3, +/−SD).

C. The capacity of 0.5μM Mirk kinase inhibitor to increase total ROS levels was measured by DCFA metabolism in SKOV3 and TOV21G ovarian cancer cells. The mean background of 9278 (+/−234) was subtracted from each sample, and then normalized to percent of untreated values in this and the following panel. Mean+/−SE shown (n=2).

D. The capacity of 0.5μM Mirk kinase inhibitor to increase total ROS levels measured by DCFA metabolism was compared in HD and BJ normal diploid fibroblasts and early passage normal human diploid ovarian (HO) epithelial cells. The mean background of 6770 (+/−258) was subtracted from each sample.

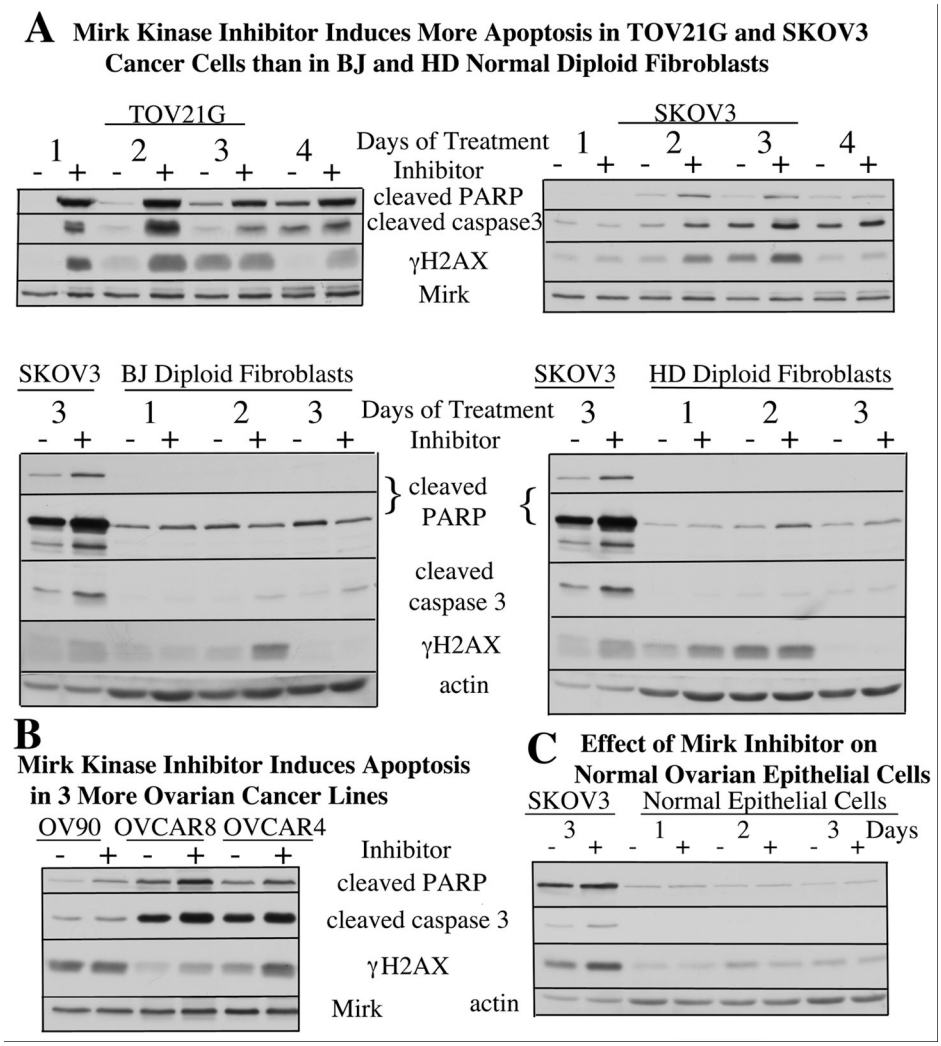

Fig. 5.

The Mirk kinase inhibitor induces apoptosis in quiescent ovarian cancer cell cultures, with little effect on normal diploid fibroblasts or normal diploid ovarian epithelial cells.

A. Time-course analyses of quiescent BJ and HD normal diploid fibroblasts and SKOV3 and TOV21G ovarian cancer cells treated with 0.5μM of Mirk kinase inhibitor. Western blotting analysis shown for the apoptosis markers cleaved PARP and cleaved caspase 3, the DNA damage marker γH2AX, Mirk and actin. (lower panels) SKOV3 cultures treated for 3 days in parallel with normal diploid fibroblasts to allow direct comparisons.

B. Similar analysis after OV90, OVCAR8 and OVCAR4 ovarian cancer cells treated for 3 days with 0.5μM Mirk kinase inhibitor.

C. Time-course western blot analysis of early passage human diploid ovarian epithelial cells for 1–3 days with 0.5 μM of Mirk kinase inhibitor, with SKOV3 cells treated in parallel in DMEM for 3 days.

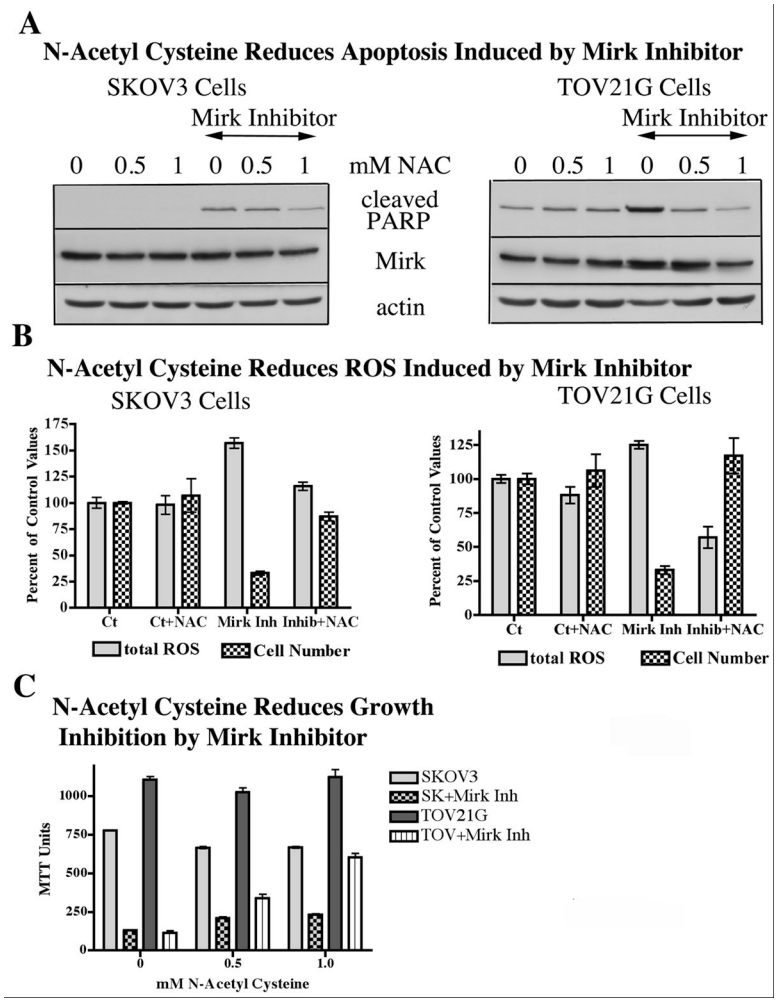

Figure 6.

The ROS scavenger N-acetyl cysteine reverses the toxicity of the Mirk kinase inhibitor towards ovarian cancer cells.

A. Quiescent SKOV3 cells and TOV21G cells were treated for 2 days with 0.5μM Mirk inhibitor, with parallel cultures also treated with 0, 0.5 or 1 mM N-acetylcysteine (NAC) the last 6 hours of incubation, before analysis by western blotting of the apoptosis marker cleaved PARP, and as controls Mirk and actin. One of 2 experiments shown.

B. Parallel cultures to those in panel “A” with 1 mM NAC were analyzed for total ROS levels by DCFA metabolism and cell numbers by direct cell counting. Similar data obtained for OVCAR3 cells (not shown).

C. Parallel cultures to panel “A” with cell numbers estimated by metabolism of MTT.